Int J Adv Manuf Technol (2009) 40:1148–1157
DOI 10.1007/s00170-008-1430-8

ORIGINAL ARTICLE

In-cycle monitoring of tool nose wear and surface roughness of turned parts using machine vision

H. H. Shahabi · M. M. Ratnam

Received: 14 June 2007 / Accepted: 4 February 2008 / Published online: 4 March 2008

Abstract Tool wear has been extensively studied in the past due to its effect on the surface quality of the finished product. Vision-based systems using a CCD camera are increasingly being used for measurement of tool wear due to their numerous advantages compared to indirect methods. Most research into tool wear monitoring using vision systems focusses on off-line measurement of wear. The effect of wear on surface roughness of the workpiece is also studied by measuring the roughness off-line using mechanical stylus methods. In this work, a vision system using a CCD camera and backlight was developed to measure the surface roughness of the turned part without removing it from the machine in-between cutting processes, i.e. in-cycle. An algorithm developed in previous work was used to automatically correct tool misalignment using the images and measure the nose wear area. The surface roughness of turned parts measured using the machine vision system was verified using the mechanical stylus method. The nose wear was measured for different feed rates and its effect on the surface roughness of the turned part was studied. The results showed that surface roughness initially decreased as the machining time of the tool increased due to increasing nose wear and then increased when notch wear occurred.

Keywords Machine vision · Tool wear · Surface roughness

1 Introduction

Tool wear and tool failure are among the limitations to unattended machining in modern manufacturing. In fact, 20% of the downtime of machine tools is reported to be due to tool failure [1]. Thus, in order to save machining costs the manufacturer has to replace worn out cutting tools 'just-in-time'. In-process (or on-line) monitoring of tool wear is therefore important in determining the best time to change the cutting tool.

Several methods of monitoring and measuring tool wear have been developed in the past. These can be broadly divided into two groups: indirect methods and direct methods. Examples of indirect methods include acoustic emission monitoring, tool-tip temperature monitoring, vibration signature analysis (acceleration signals), monitoring of motor current, and cutting force monitoring [2]. These methods normally require expensive instrumentation and are difficult to implement in a typical workshop environment. Direct methods, such as machine vision systems using a charged-couple-device (CCD) camera or optical microscope, are able to measure tool wear directly. They are simpler and require less costly equipment compared to the indirect methods. Therefore, the application of machine vision to measurement of tool wear has been of great interest in the research community in recent years [1, 3–14].

The effect of tool wear on the surface quality of machined parts is well known [13–14]. The ease of capturing and analyzing images of machined surfaces has encouraged researchers in the past to use roughness parameters for tool wear monitoring. Analysis of surface texture is one method of distinguishing a sharp tool from a worn out tool [12]. The surface roughness can also be measured directly using mechanical stylus methods. Although the stylus method is accurate it has several disadvantages. For example, the stylus and its transducer are delicate and thus the instruments must be used in a fairly vibration-free environment, and the method is slow

H. H. Shahabi · M. M. Ratnam (✉)
School of Mechanical Engineering, Engineering Campus,
Universiti Sains Malaysia,
14300 Nibong Tebal, Penang, Malaysia
e-mail: mmaran@eng.usm.my

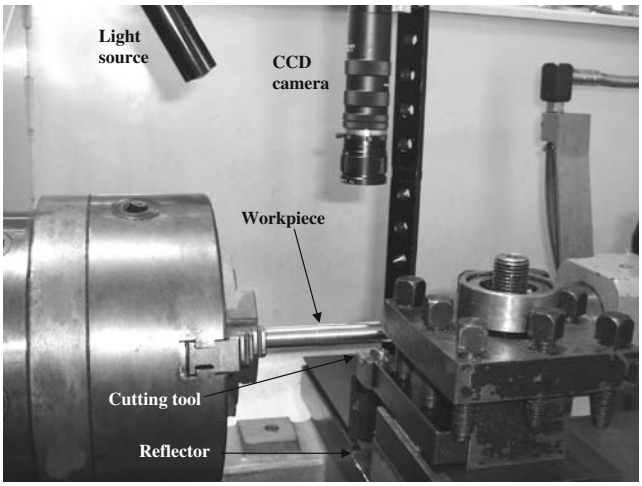

Fig. 1 System setup on lathe machine

and not suitable for in-cycle measurement of roughness in the workshop area.

In-process monitoring of surface roughness is important because the effect of tool wear on surface finish can be assessed directly. Although many optical methods for measuring tool wear and surface roughness have been proposed in the past, these methods either require the tool or the workpiece to be removed from the machine and inspected in the laboratory. In this research, a vision system has been developed for the measurement of surface roughness of the workpiece in turning operations within the workshop area. The measurement is carried out in-between cutting processes, i.e. in-cycle, without removing either the cutting tool or workpiece from the machine.

2 System configuration

2.1 System setup

The system used for measuring the tool wear and surface roughness is shown in Fig. 1. A high-resolution (1392×1040 pixels) CCD camera (JAI CV-A1) was used to capture the images of the cutting tool and workpiece. The camera was fitted with a 50 mm lens (model GMHR35028MCN; Goyo Optical Inc., Japan) for measuring tool wear area and a 25 mm lens (model GMHR32514MCN) for measuring workpiece roughness. A 110 mm extension tube was fitted to increase the optical magnification. Backlighting was used to capture the contour of the cutting tool and workpiece. The position of the camera was adjusted so that either the cutting tool or workpiece surface could be captured. The use of the 50 mm lens resulted in a larger field-of-view due to the increase in object-to-lens distance. Since the use of a long extension tube could result in image

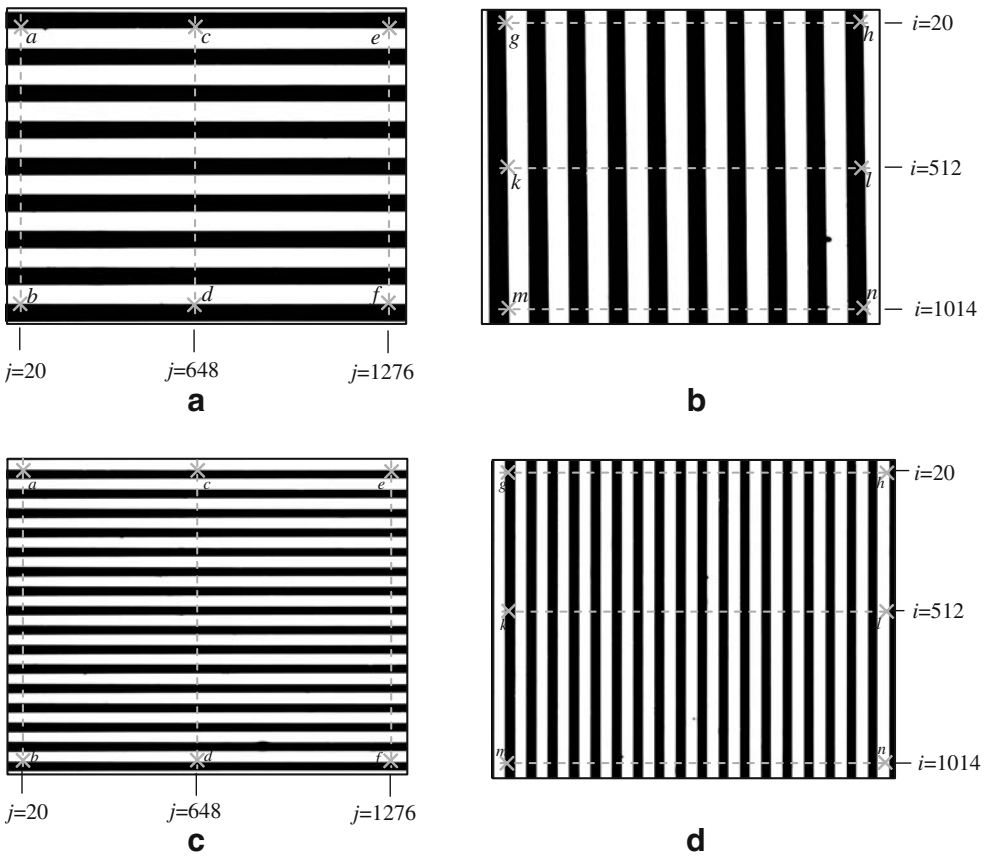

Fig. 2 Images of Ronchi rulings. **a**, **b** 25 mm lens. **c**, **d** 50 mm lens

Table 1 Distances between measurement points on image (see Fig. 2) (pixels)

Points	Lens focal length	
	25 mm	50 mm
a-b	898	949
c-d	899	949
e-f	898	948
g-h	1097	1228
k-l	1098	1228
m-n	1096	1228

distortion, the presence of distortion was checked using high precision Ronchi rulings having 200 lines per inch (Edmund Optics Pte. Ltd., Singapore). Separate images of the rulings placed in horizontal and vertical positions were captured using the 25 mm and 50 mm lenses. The images were contrast enhanced and scanned at various points shown in Fig. 2a–d. The distances between these points were calculated to assess the amount of distortion. The results in Table 1 show that maximum difference in distance between the points is 2 pixels (0.18%). Since the output of the CCD camera is in pixels and the surface roughness of the workpiece must be determined in μm, it was necessary to determine the horizontal and vertical scaling factors in mm/pixel. These factors were obtained using pin gages of known dimensions and are shown in Table 2.

2.2 Machining condition

Several parameters can influence the surface roughness of the workpiece and tool wear. These include machining duration, cutting speed, feed rate, properties of cutting tool, material of workpiece, and properties of coolant. Table 3 shows the parameters used in this study.

3 Description of measurement algorithm

The various stages of the measurement of workpiece roughness are shown in Fig. 3 and are described in the following sub-sections. Detailed description of the algorithm used for tool wear measurement is published separately [15].

Table 2 Horizontal and vertical scale factors

Lens focal length	Direction	Scaling factor (μm/pixel)	Field of view of camera
50 mm	Horizontal	1.81	2.3 mm×2 mm
	Vertical	2	
25 mm	Horizontal	1	1.3 mm×1.1 mm
	Vertical	1.06	

Table 3 Machining parameters

Machine tool	Conventional lathe (Harrison 600; The 600 Group, UK)
Workpiece	Stainless steel rod, AISI308
Cutting tool	Uncoated cemented carbide: TPUN-16–03–04_H13A (Sandvik Co, Ltd, Sweden)
Feed rate	0.2, 0.25, 0.3, 0.4 mm/rev
Machining depth	0.5 mm
Cutting speed	58 m/min
Coolant	Air
Machining time	5, 25, 50, 75, 100, 125, 150,175, 208 min

3.1 Image acquisition

In the stage 1, a frame-grabber (DT3162; DataTranslation, Inc., USA) was used to interface the CCD camera to the computer. The frame grabber is a digitizer that acts as an image buffer. Output of the CCD camera was captured and digitized using this frame grabber.

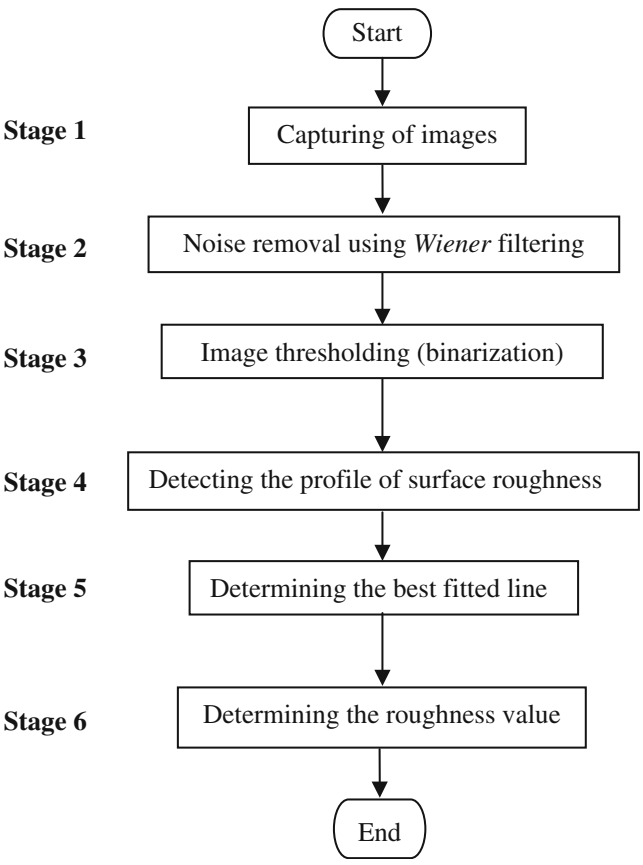

Fig. 3 Flowchart of algorithm for roughness measurement

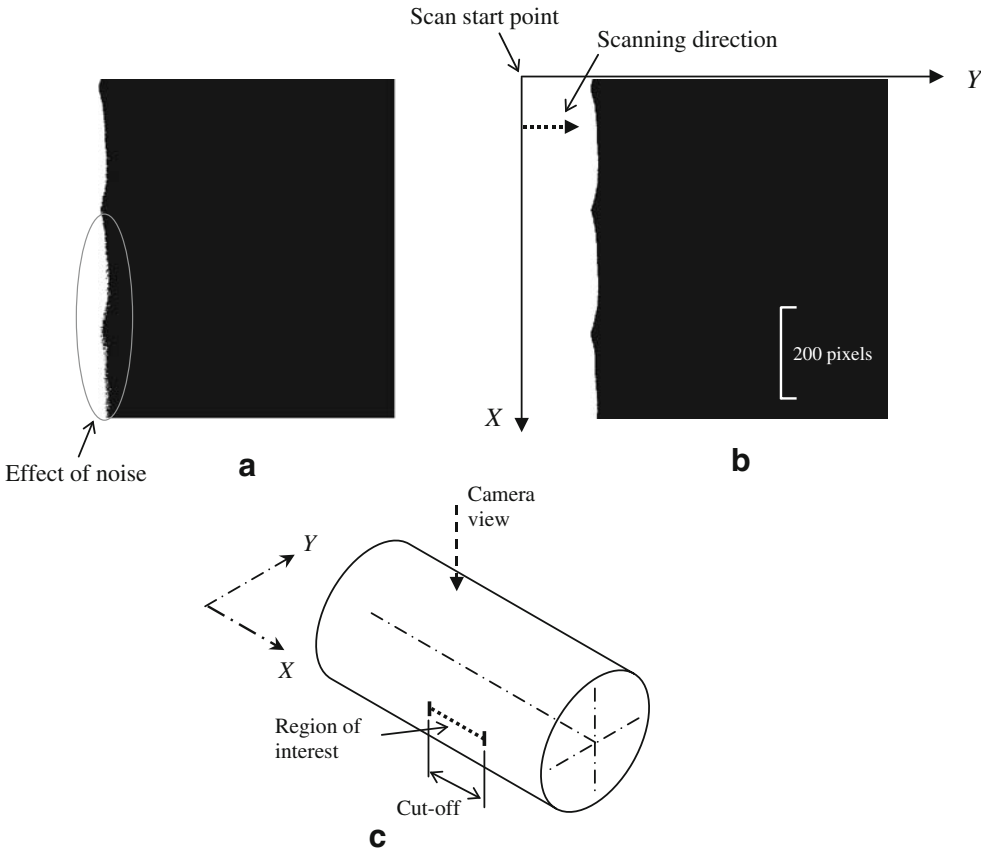

Fig. 4 Images of surface roughness profile. **a** Before Wiener filtering. **b** After Wiener filtering. **c** Region where surface profile is captured

3.2 Image enhancement

In stage 2, the images were enhanced using noise filtering methods. The captured image $g(x,y)$ can be represented by [16]:

$$g(x,y) = h(x,y)*f(x,y) + \eta(x,y) \quad (1)$$

where $f(x,y)$ is the original image, $h(x, y)$ is the degradation function, $\eta(x,y)$ is the additive noise term in the image and the asterisk refers to the convolution operation. Wiener filtering was used to recover the images that were degraded by noise [16, 17]. The Wiener filtering method, introduced in 1942, is not sensitive to inverse filtering of noise and is one of the best approaches to recover images. The Wiener filter uses statistical parameters to minimize error. Although it is normally used to restore blurred images, Matlab uses this method to enhance images affected by noise using the wiener2 command. This command does not need to have any information about the noise distribution and applies the Wiener filter adaptively using the local statistical parameters. Compared to a linear filter, the Wiener filter is more selective and preserves edges and other high frequency components in the image. Figure 4a,b shows sample images of workpiece contour before and after Wiener filtering. Figure 4c shows the view direction of the camera relative to the workpiece and the region where the roughness profile is captured.

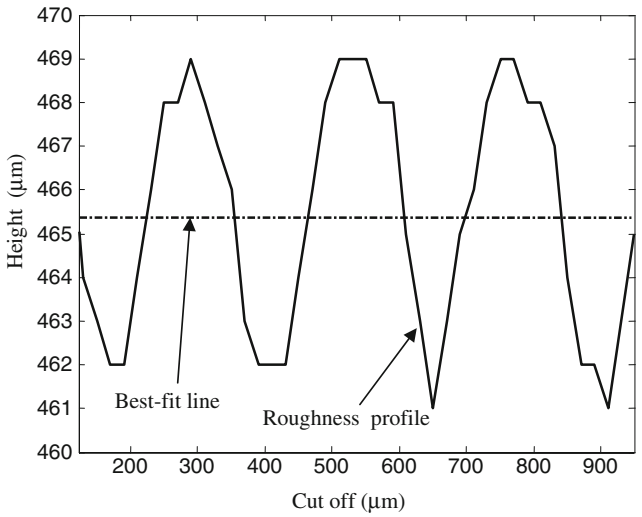

Fig. 5 Contour of roughness profile

3.3 Segmentation

In stage 3, the image was segmented to separate the workpiece (dark region) from its background (bright region) using a global thresholding method. Thresholding produces a binary image by setting all pixels in the input image for a given range of gray values to 1 and the remaining values to 0. The threshold value T is used to define

Table 4 Comparison between roughness determined using vision method and stylus method

Cutting speed (m/min)	Feed rate (mm/rev)	$R_a(v)$ μm	$R_a(s)$ μm	$\frac{\lvert R_a(s)-R_a(v)\rvert}{R_a(s)}$ (×100%)	$R_q(v)$ μm	$R_q(s)$ μm	$\frac{\lvert R_q(s)-R_q(v)\rvert}{R_q(s)}$ (×100%)
16.3	0.2	1.81	1.75	3.4%	2.14	2.10	1.9%
	0.25	2.50	2.62	4.6%	2.87	3.03	5.3%
	0.3	3.25	3.23	0.6%	3.73	3.77	1.1%
	0.4	5.23	4.95	5.7%	6.28	6.04	4.0%
23.8	0.2	1.72	1.76	2.3%	2.00	2.18	8.3%
	0.25	2.96	2.69	10.0%	3.41	3.13	9.0%
	0.3	3.38	3.49	3.2%	3.97	4.10	3.2%
	0.4	6.82	6.70	1.8%	8.02	7.78	3.1%
39.6	0.2	1.74	1.76	1.1%	2.06	2.18	5.5%
	0.25	2.58	2.67	3.4%	3.06	3.23	5.3%
	0.3	2.61	2.64	1.1%	3.11	3.15	1.3%
	0.4	6.48	6.42	0.9%	7.66	7.63	0.4%

$R_a(v)$ and $R_q(v)$: Roughness determined using vision method.
$R_q(s)$ and $R_q(s)$: Roughness measured using stylus method.

the range of grayscale values that are set to 0 and 1. T was determined automatically using the "graythresh" command in Matlab that uses the well-known Otsu's method [18]. Otsu's algorithm uses the image histogram to determine the threshold value. The algorithm assumes that the image histogram is bimodal and determines the optimum threshold value that separates the two groups of pixels.

3.4 Roughness measurement

The captured image shows the workpiece surface contour and the roughness value can be determined directly from the image without the need of a stylus method. In stage 4, the surface contour in the binarized image was detected using an algorithm written in Matlab. Each image is read as a matrix of X and Y (row by column). Since in the binarized images, white areas have an intensity value of 1 and black areas have an intensity value of 0, the surface profile of the workpiece is detected when the intensity value changes from 1 to 0. The algorithm starts scanning from the first pixel of the first column. If the first pixel value is 0 the scanning stops and begins at the second row. If it is not 0 it checks the second pixel in the same row. This operation continues to search for a 0 pixel in the first row. Then, the first 0 value pixel of the second row is searched. This scanning is repeated for all the rows to detect the contour of the surface roughness profile.

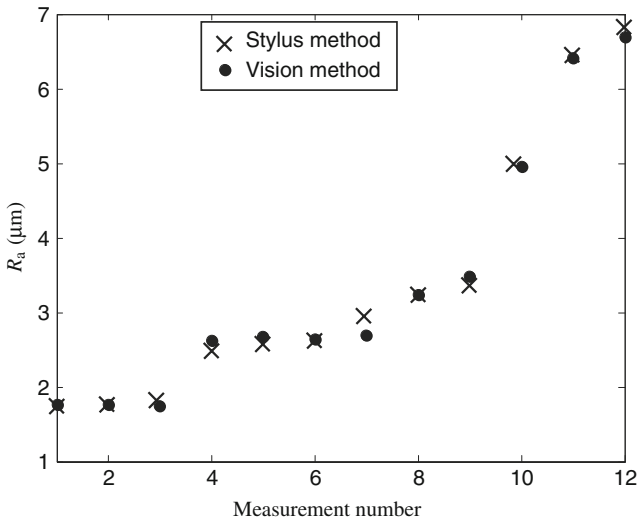

Fig. 6 Comparison between roughness determined using the vision method and the stylus method

A typical profile is shown in Fig. 5. Since the detected roughness profile is in pixels, the scaling factors obtained earlier were used to convert the roughness to micrometers. The surface roughness can be determined by subtracting the mean value of the roughness profile from each point on the contour. In the fifth stage the best-fit line of the detected contour, considered as a mean line, was determined. The best fitted line is also shown in Fig. 5.

In stage 6, two amplitude parameters, the centerline average (R_a) and root mean square (R_q), which are the most common parameters of the roughness test, were determined. R_a and R_q are difficult to measure directly but their reliability are higher compared to other roughness parameters. If equal spaces of horizontal distances, assumed as 1,2,3,…n, have respective absolute heights h_1,h_2,h_3,h_4,...,h_n, then [19]

$$R_a = \frac{h_1 + h_2 + h_3 \ldots + h_n}{n} = \frac{1}{n}\sum_{i=1}^{n} h_i \tag{2}$$

$$R_q = \sqrt{\frac{h_1^2 + h_2^2 + h_3^2 \ldots + h_n^2}{n}} = \sqrt{\frac{\sum_{i=1}^{n} h_i^2}{n}} \tag{3}$$

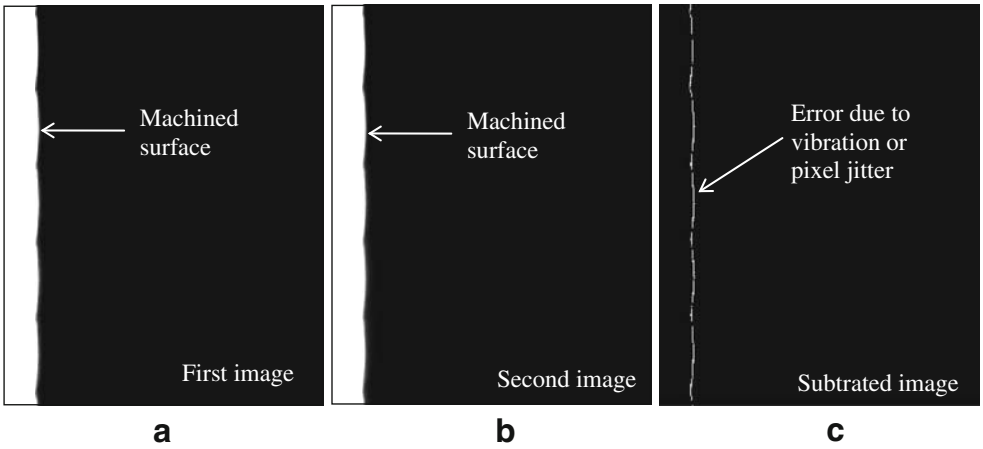

Fig. 7 Images of surface roughness profile in the presence of ambient vibration. **a** First image. **b** Second image. **c** Subtraction of images in **a** and **b**

In this work, n is equal to the length of the image in pixels along the roughness profile.

4 Results and discussion

4.1 System verification

4.1.1 Surface roughness measurement using a CCD camera

To prepare the workpiece, an uncoated carbide insert was used to machine a stainless steel rod. The workpiece was removed from the lathe machine and 16 images of the workpiece surface contour were captured at various locations using the vision system. The average value of R_a and R_q of these 16 images were calculated from the profiles extracted using the algorithm described earlier. This was repeated for 12 different workpieces under different cutting speeds and feed rates shown in Table 4.

A roughness tester (model SJ-201P; Mitutoyo) was used to verify the results of roughness measured using the vision system. Each surface was measured 16 times in different regions of the workpiece. Table 4 also shows the results of surface roughness measurement and comparison with the mechanical stylus method. The results show that the maximum deviation for R_a and R_q between vision and stylus methods are, respectively, 10% and 9%. Figure 6 show a plot of R_a versus measurement number determined using the vision method and stylus measurement. The comparison shows that the vision method is able to provide reliable roughness values.

4.1.2 Effect of ambient lighting

To study the effect of ambient lighting on the system error, 16 images of one region of a workpiece were captured under different ambient light intensities. A light meter (Lx-101A, LT Lutron) was used to record the ambient light intensity. The light intensity was varied between 12 lux and 1935 lux. The surface roughness of all 16 profiles was determined to evaluate the system error due to different ambient light intensities. The mean values of R_a and R_q for 16 images due to the different light intensities were found to be 1.81 μm and 2.20 μm. The maximum deviations between the 16 values were 2.1% and 2.2% for R_a and R_q, respectively.

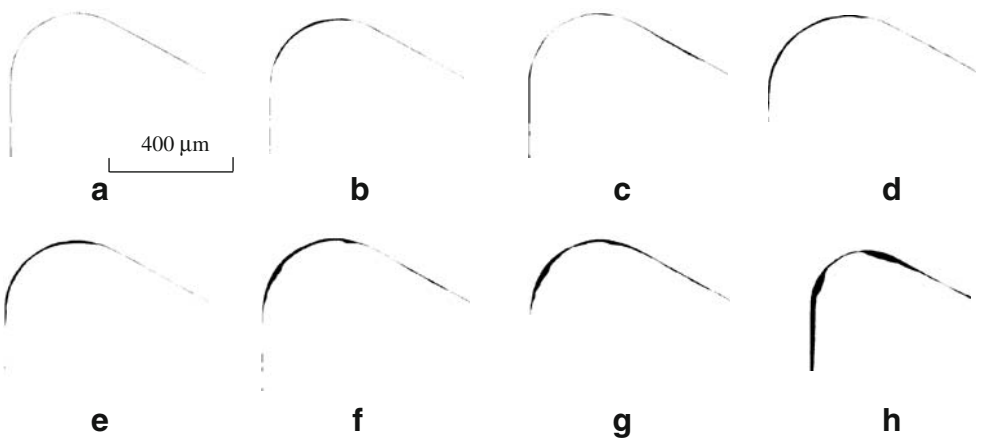

Fig. 8 Images of cutting tool wear area. **a** After 5 min. **b** After 25 min. **c** After 50 min. **d** After 75 min. **e** After 100 min. **f** After 125 min. **g** After 175 min. **h** After 208 min

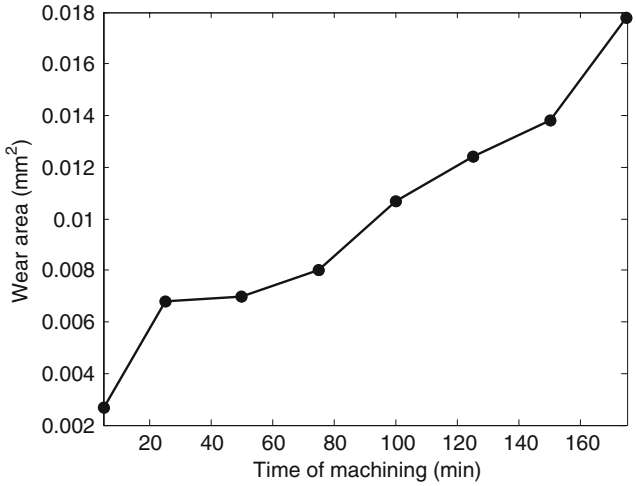

Fig. 9 Plot of cutting tool wear area vs. machining time

4.1.3 Effect of vibration

To study the effect of vibration in the environment on the measured roughness, 16 different images of one region of a workpiece were captured under the same lighting condition. Since the workpiece was not moved, any difference between images could be due to ambient vibration, changes caused by thermal effects, or pixel jitter during image capture. Since the experiment was carried out under room temperature conditions the difference is mostly likely due to vibration or pixel jitter. Figure 7a,b shows two images of the workpiece profile and Fig. 7c is their subtraction result. The white pixels in the figure after subtraction show the effect of vibration or pixel jitter. The surface roughness of 16 images of the workpiece profile was determined to investigate the effect of these errors.

The average values of R_a and R_q of the 16 images in the presence of different ambient vibration were found to be 1.84 and 2.24 μm, respectively. The deviations between the 16 values of R_a and R_q determined using the vision method are 1.99% and 0.8%, respectively. Since this deviation is small the system can be considered as unaffected seriously by environmental disturbances.

4.2 Tool wear and its effect on surface roughness

4.2.1 Tool wear measurement

The images of the cutting tool show the tool contours and from these images the area of the cutting tool tips can be determined. When the cutting tool tips are worn, the area of the tool tip decreases. By subtracting the images of worn and unworn tools the wear area can be determined. Figure 8a–h shows eight images of tool wear areas for machining time between 5 and 208 minutes. The subtraction was carried out after applying a conforming method that corrects misalignment between the images [15]. This method corrects misalignment in the cutting tool using the captured images. The wear area was determined by finding the area of the subtracted image (in pixels) and multiplying it by the horizontal and vertical scaling factors given in Table 2. Figure 9 shows a plot of wear area against machining time where the wear area increases gradually between 5 and 175 minutes.

4.2.2 Effect of tool wear on surface roughness

To study the effect of tool wear on surface roughness the workpieces were machined using the worn cutting tool. The machining parameters are given in Table 3. For each workpiece 16 images of surface roughness profiles were captured. Figure 10a–d shows the images of workpiece profiles for different machining times, and Fig. 11a–d shows the corresponding roughness plots. The images shown in Fig. 10a–d were captured from workpieces machined with feed rates of 0.2 mm/rev. The surface roughness initially decreased and then increased after a certain machining time. A study of other images captured from the workpieces prepared using feed rates of 0.25, 0.3,

Fig. 10 Images of workpiece profile. **a** New tool. **b** After 50 min. **c** After 75 min. **d** After 175 min

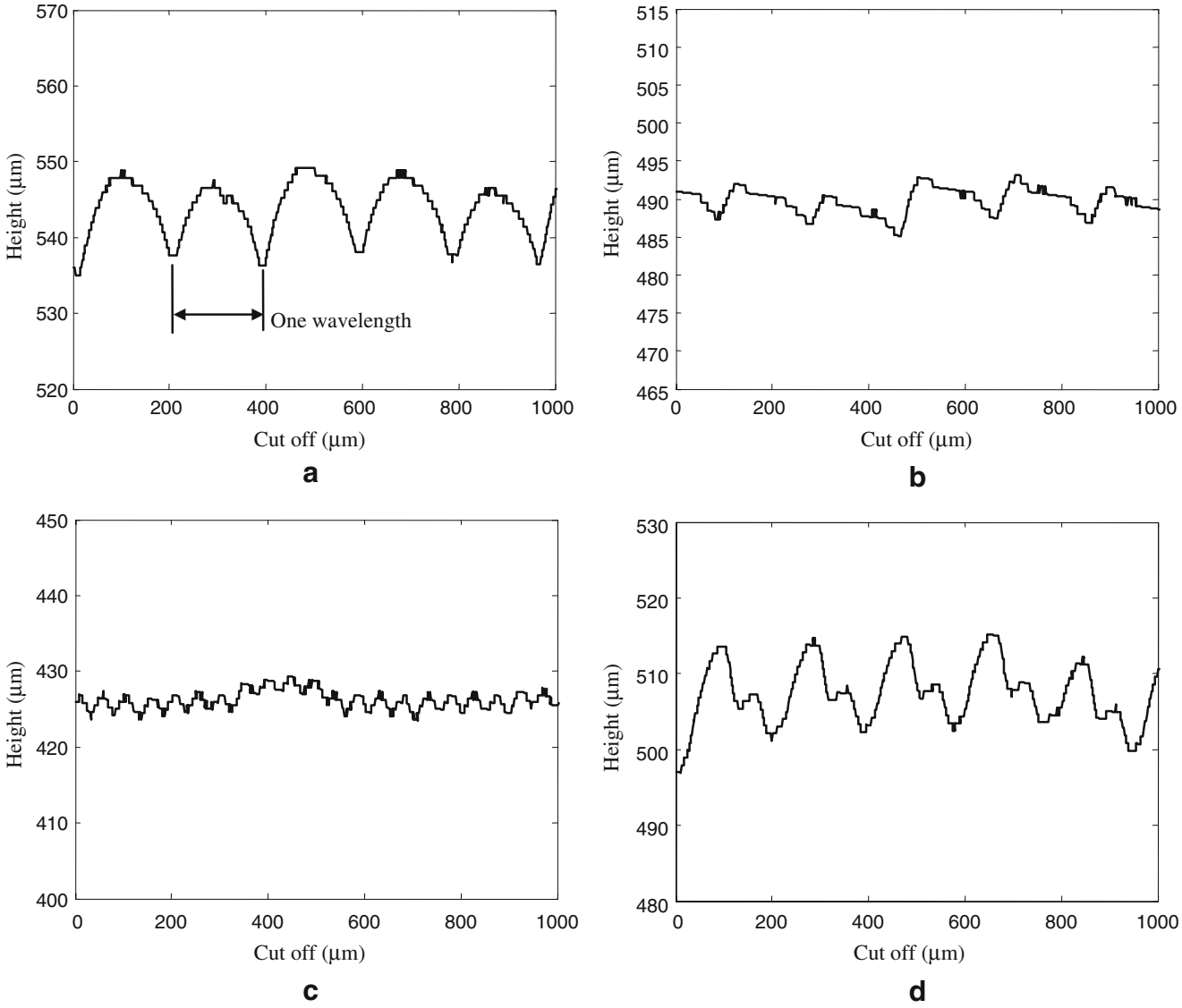

Fig. 11 Roughness profiles of workpiece. **a** New tool. **b** After 50 min. **c** After 75 min. **d** After 175 min

and 0.4 mm/rev also revealed similar trends. The reason for this can be explained by plotting the workpiece surface profiles.

As Fig. 11a–d shows, the surface profile is repeating more or less periodically as expected and horizontal length of each cycle is nearly equal to the machining feed per revolution (0.2 mm). The fluctuation in the periodic profile in some of the cases is due to disturbances in the machining process because the maximum fluctuation is less than 5 μm. The 'period' of each profile does not change when the machining time is increased, rather only the amplitude changes. When the cutting tool is new (sharp) the roughness is maximum and when the tool is used for some time the roughness decreases. This is due to increasing nose wear that causes a smearing effect on the workpiece. This phenomenon continues until a machining time of approximately 75 min for feed rates of 0.25 mm/rev and 0.3 mm/rev. After 100

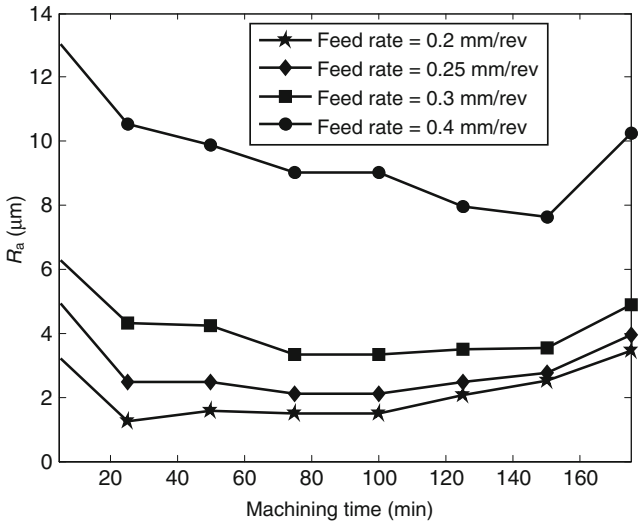

Fig. 12 Effect of feed rate and machining time on R_a

minutes of machining time the roughness increases and continues to increase until the cutting tool breaks or is badly worn (175 min). Figure 12 shows the variation of surface roughness with machining time determined using the machine vision system. When the feed rate is higher, the roughness value is greater at any machining time.

One wavelength of roughness profile for each machining time was used to study the roughness profile more closely (Fig. 13a–d). Each of the roughness profiles was plotted using the same scale in the horizontal and vertical axes. Comparison of cutting tool geometry and wavelength of roughness profile shows a close correlation between the two. The gradual growth of nose wear causes flattening of the roughness profile and therefore the surface roughness decreases. However, the growth of notch wear causes changes to the shape of the roughness profile to a less flattened shape (Fig. 13d) and therefore the roughness increases.

In previous research, Choudhury et al. [3] reported that when flank wear increases the roughness value decreases. Kassim et al. [2] also described that the surface roughness decreases as flank wear increases if the influence of flank wear is predominant. They reported that flank wear is predominant at the initial stage of tool wear, but in the second stage other types of wear such as notch wear and crater wear have greater effects on surface roughness, though the reason for this observation was not clear. However, flank wear is not a reliable parameter when a

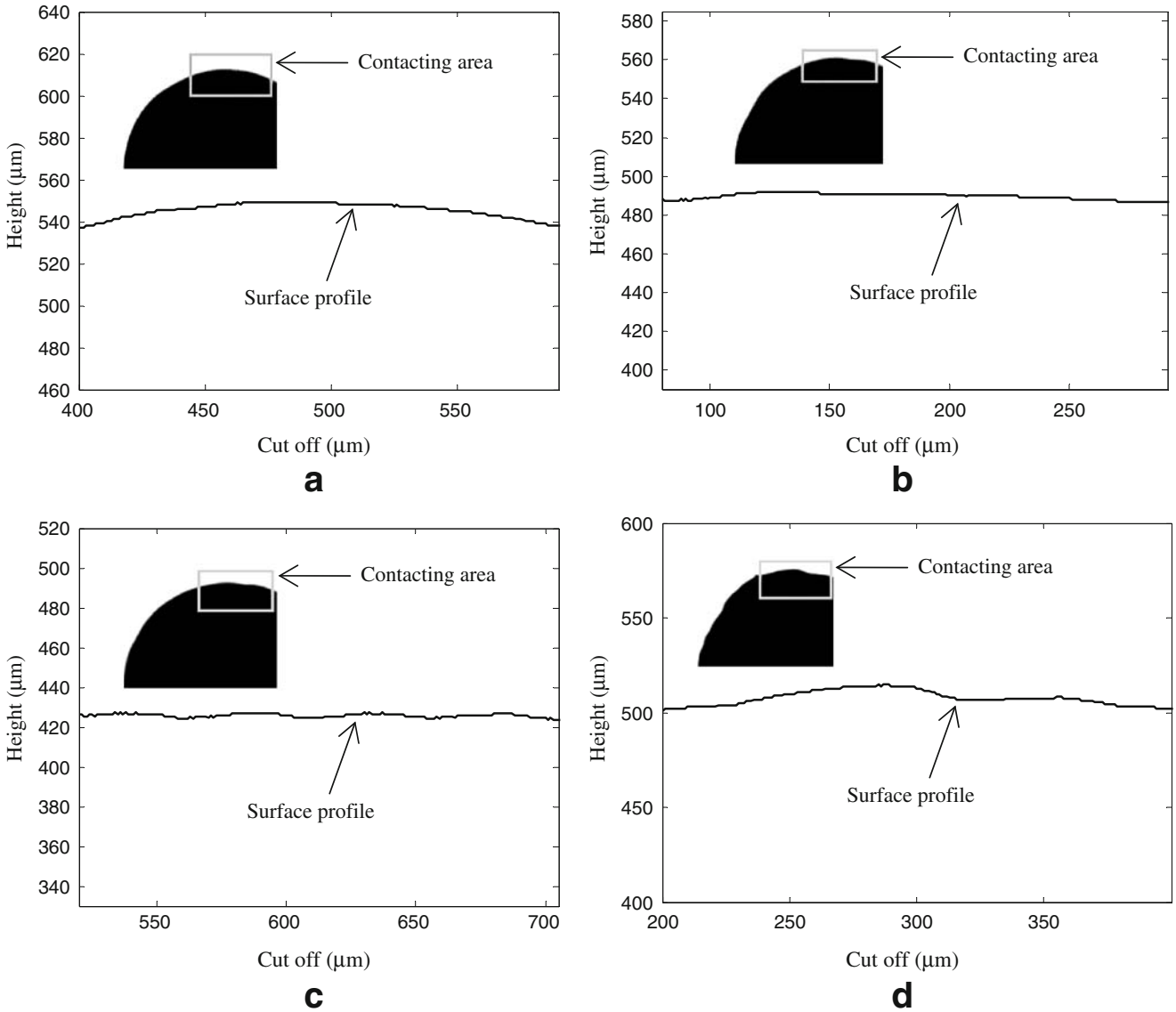

Fig. 13 Comparison between cutting tool profile and workpiece surface profiles for one wavelength. **a** New tool. **b** After 50 min. **c** After 75 min. **d** After 175 min

surface roughness requirement has to be met [19, 20]. In a similar study, Pavel et al. [13] reported that when the output of a machining process is continuous chip the roughness value increased with machining time. When the chip is not continuous the roughness value decreased with machining time. When notch wear is negligible the surface roughness decreases with flank wear, and when notch wear increases the roughness value increases. This was, however, not confirmed experimentally in their paper. The results of our study show that increasing flank wear flattens the tool nose area and this decreases the surface roughness of the workpiece. However, increasing notch wear after 75 minutes of machining time increases the roughness value. The machine vision system developed in this work can be extended to further study the effect of nose wear on workpiece surface roughness under other machining conditions, such as different workpiece materials and cutting speeds.

5 Conclusion

The noncontact method using machine vision proposed in this work and in previous work [15] enables the measurement of both cutting tool nose wear area and surface roughness of turned parts using the same setup. An algorithm that employs Wiener filtering and simple thresholding on backlit images reduces errors caused by the environmental factors such as ambient lighting and vibration. A comparative study using the stylus method of roughness measurement showed that the maximum deviation in roughness value measured using the proposed system is about 10%. A study of 2D tool wear area using the system developed shows that increasing the feed rate increases the surface roughness if other machining parameters are not changed. Also, the results show that increasing the machining time of the tool decreases the surface roughness in the first stage of machining due to increase in nose wear. However, in the second stage of machining (after 75 minutes), the roughness value increases due to the effect of growing notch wear.

The surface profiles of the workpiece show that roughness is periodic as expected, and this was clearly visible at different machining times. A close correlation was found to exist between the shape of the wear area of the cutting tool and the roughness profile. The system and measurement algorithm developed can be applied within the workshop environment for the in-cycle monitoring of tool wear and workpiece surface roughness.

Acknowledgement The authors wish to thank Universiti Sains Malaysia for the short-term grant that enabled this study to be carried out.

References

1. Kurada S, Bradley C (1997) A review of machine vision sensors for tool condition monitoring. Comput Ind 34:55–72
2. Kassim AA, Mian Z, Mannan MA (2004) Connectivity oriented fast Hough transform for tool wear monitoring. Pattern Recogn 37:1925–1933
3. Choudhury SK, Bartarya G (2003) Role of temperature and surface finish in predicting tool wear using neural network and design of experiments. Int J Mach Tools Manuf 43:747–753
4. Sortino M (2003) Application of statistical filtering for optical detection of tool wear. Int J Mach Tools Manuf 43:493–497
5. Pfeifer T, Wiegers L (2000) Reliable tool wear monitoring by optimized image and illumination control in machine vision. Measurement 28:209–218
6. Lanzetta M (2001) A new flexible high-resolution vision sensor for tool condition monitoring. J Mater Process Technol 119:73–82
7. Yang MY, Kwon OD (1996) Crater wear measurement using computer vision and automatic focusing. J Mater Process Technol 58:362–367
8. Wang WH, Hong GS, Wong YS (2006) Flank wear measurement by a threshold independent method with sub-pixel accuracy. Int J Mach Tool Manu 46(2):199–207
9. Kurada S, Bradley C (1997) A machine vision system for tool wear assessment. Tribology Int 30(4):294–304
10. Jurkovic J, Korosec M, Kopac J (2005) New approach in tool wear measuring technique using CCD vision system. Int J Mach Tools Manu 45:1023–1030
11. Dawson TG, Kurfess TR (2005) Quantification of tool wear using white light interferometry and three-dimensional computational metrology. Int J Mach Tool Manu 45:591–596
12. Mannan MA, Kassim AA, Jing M (2000) Application of image and sound analysis techniques to monitor the condition of cutting tools. Pattern Recogn Lett 21:969–979
13. Pavel R, Marinescu J, Deis M, Pillar J (2005) Effect of tool wear on surface finish for a case of continuous and interrupted hard turning. J Mater Process Technol 170:341–349
14. Tamizharasan T, Selvaraj T, Noorul Haq A (2006) Analysis of tool wear and surface finish in hard turning. Int J Adv Manuf Technol 28:671–679
15. Shahabi HH, Ratnam MM (2007) On-line monitoring of tool wear in turning operation in the presence of tool misalignment. Int J Adv Manuf Tech. DOI 10.1007/s00170-007-1119-4
16. Gonzalez RC, Woods RE, Eddins SL (2004) Digital image processing using Matlab. Pearson-Prentice Hall, New Jersey
17. Lim JS (1990) Two-dimensional signal and image processing. Prentice Hall, Englewood Cliffs, NJ, pp 536–540
18. Otsu N (1979) A threshold selection method from gray-level histograms. IEEE Trans Syst Man Cybern 9(1):62–66
19. Gayler JFW, Shotbolt CR (1990) Metrology for engineers. Cassell, London
20. Kwon Y, Fischer GW (2003) A novel approach to quantifying tool wear and tool life measurements for optimal tool management. Int J Mach Tool Manu 43:359–368